

Quark Matter 99 Summary: Hadronic Signals

R. Stock

Physics Department, University of Frankfurt, D-60486 Frankfurt

1 Introduction

It was obvious at this conference that the heavy beam program at the AGS (Au) and at the SPS (Pb) has been completely successful, all experiments delivering the physics that they were built for. We have been presented such a wealth of beautiful precision data (from the AGS in particular) that no summary can give proper credit to everybody. Neither is the restriction to "hadronic signals" helpful in reducing the scope because, with the exception of direct photons and lepton pair continua we have been discussing hadron production throughout. In fact the long standing discussion of threshold effects in charmonium production, upon variation of impact parameter and/or system size has inspired a comprehensive program of similar searches for "onset" phenomena in bulk hadron production data. This will be my first major topic: look at the evolutions with system size (from $p+p$ via either intermediate mass nuclei or semiperipheral collisions to central mass 200 collisions) and with \sqrt{s} . I will then turn to the progress in understanding the differences between the two major decoupling stages during expansion: first from inelastic interactions ("chemical freezeout"), later on from resonance decay and elastic interaction ("global freezeout"). Starting with the latter the progress concerning the evidence for collective transverse velocity fields will be reviewed. In the final section I will discuss how the chemical freezeout stage (that fixes the hadronic production rates and their ratios) is intimately related to the QCD hadronization process, leading to the conclusion that analysis of such data in central $Pb+Pb$ collisions at $\sqrt{s} = 17 GeV$ reveals the position of the parton to hadron phase transformation in temperature, energy density and baryochemical potential.

2 New types of data

Before engaging with the heavy systematics announced above I wish to mention a few highlights of data pointing beyond the presently well-discussed physics. Of course a strictly subjective choice, with advance apologies to the unavoidable omissions.

Fig. 1 shows the combined WA98 [1] and NA45 [2] data for identified pions in central $Pb+Pb$ collisions at top SPS energy. The transverse mass scale ranges up to $4 GeV$, far beyond the domain in m_T on which we normally base our arguments concerning thermal or radial flow model inspired inverse slopes. Actually the local inverse slope parameters vary throughout the scale due to the overall concaveness, a warning with regard to flow model interpretation of pion spectral data but, on the other hand, perhaps the first glance at hard partonic scattering in SPS $A+A$ collisions - a topic emphasized by Gyulassy [3] for future RHIC physics of jet attenuation etc.. We thus expect to see these data in a new light at QM 2000.

Turning to pion Bose-Einstein correlations the review talk by Wiedemann [4] discussed the very indirect way in which straight forward geometrical source size reflects in the data. But some confidence in a naive geometrical interpretation is regained from E895 results for semi-central $Au+Au$ collisions [5]. Fig. 2 shows the data for the "sideward

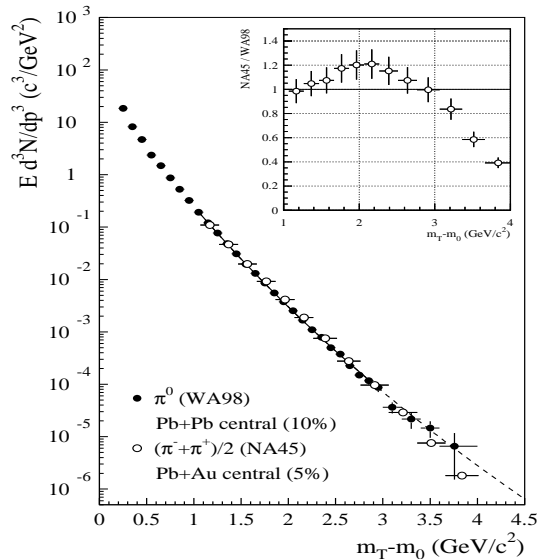


Figure 1: Identified pion transverse mass spectrum from WA98 [1] and NA45 [2] for central $Pb + Pb$ collisions at $158 \text{ GeV}/A$.

radius" R_s which was determined (for the first time) differentially, in azimuthal orientation relative to the eventwise reaction plane. Intuitively the reaction fireball should look large as it is seen head-on, and small(er) looking edge-on; and it does. Further evidence that HBT analysis can be applied to single events and their source geometry (and not only to ensemble averages of thermally coherent subvolumes, terms with which the hydrodynamical models [6] frighten the practitioner) is given by Fig. 3. The first (preliminary) event-by-event analysis of central $Pb + Pb$ collisions by NA49 [7] shows an approximately symmetric distribution of the eventwise radius, the maximum well corresponding to the ensemble average [8] of $R_{inv} = 7.5 \text{ fm}$. We shall learn more about this signal from experiment STAR at RHIC but note, for the time being, that the width of the distribution, and even the slight indication of an asymmetry toward large R are roughly consistent with expectation from considering pair counting statistics at fixed radius [9]; i.e. there seem to be no prominent source volume fluctuations. At RHIC a more informative analysis (in terms separately of longitudinal and transverse source geometry) should prove feasible.

Related to HBT but much less developed theoretically is the geometrical information derived from fireball nucleon coalescence into light clusters. The deuteron or anti-deuteron coalescence factor [10] $B_2 = [d]/[p]^2$ is expected to fall down with increasing source size and temperature (as well as with nucleon pair transverse mass as shown by NA44 [11]), and the systematics has now reached a perfect level by AGS E866 [12], E864 [13], SPS NA44 [11] and NA52 [14]. However, completely striking was the vast extension of coalescence physics by E864, both to heavier and metastable nuclear species and to light hypernuclei [13,15]. Fig. 4 illustrates their data for coalescence systematics up to ${}^7\text{Be}$, with yield smaller by about 8 orders of magnitude than for the deuteron. Normalizing away the overall exponential law there remains a dependence on the cluster binding

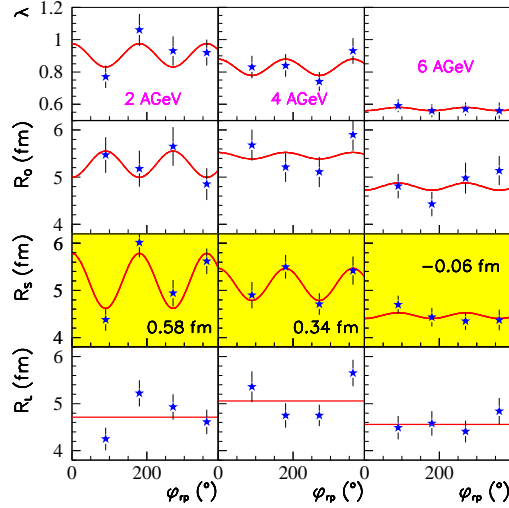


Figure 2: HBT pion pair analysis by E895 [5] of semiperipheral $Au + Au$ collisions, showing dependence of source parameters relative to the eventwise reaction plane.

energy per nucleon (i.e. the nucleon density). Will we next see exotic halo nuclei within hot coalescence rather than cold fragmentation? E864 shows more interest in the exciting physics of light hypernuclei measuring the yield ratio of hyper-tritium to 3He [15]. This entire field is special to the AGS program.

3 Evolution with centrality and \sqrt{s}

A decade of experimental search for the dependence of charmonia (J/ψ and ψ^*) yields on system size and energy density [16] has made us aware of threshold effects modifying a smooth or even constant yield of some species relative to the number of colliding baryon participants, or the total transverse energy in the colliding system. Search for such changes with increasing energy density was motivated by the QCD-Debye-screening model of Matsui and Satz [17] which introduced discussion of several characteristic steps in the energy density: if the transition from hadronic matter to a quark gluon plasma was assumed at $T = T_{crit}$ and corresponding energy density ϵ_{crit} , then the QCD screening mechanism dissolves first the ψ^* and χ states, at $T \approx 1.1T_c$, then J/ψ at $T \approx 1.3T_c$ and, much later, the bottomonium Y at about $2.5 T_c$. Thus in this highly idealized, schematic model there is a sequence of characteristic thresholds; the J/ψ , in particular, would disappear at $\epsilon \approx 2.8 \epsilon_{crit}$ as ϵ is proportional to T^4 from lattice QCD [18]: i.e. **well above the critical energy density!** At this conference the NA50 Collaboration has shown a dramatic final drop in the J/ψ yield occurring at the most central $Pb + Pb$ collisions at $\sqrt{s} = 17 GeV$. Let us for a moment accept that this signals J/ψ screening, and that this occurs at $\epsilon \approx 3 \epsilon_{crit}$ (in spite of the very intense ongoing discussion). Recall the Bjorken estimate of the average (transverse) energy density in the primordial reaction volume: for central $Pb + Pb$ it is $\epsilon \approx 3 GeV/fm^3$ from NA49/WA87 calorimetry [19]. This finally leads to the estimate $\epsilon_{crit} \approx 1 GeV/fm^3$, in accord with recent lattice

NA49 Pb+Pb Event-by-Event HBT (PRELIMINARY)

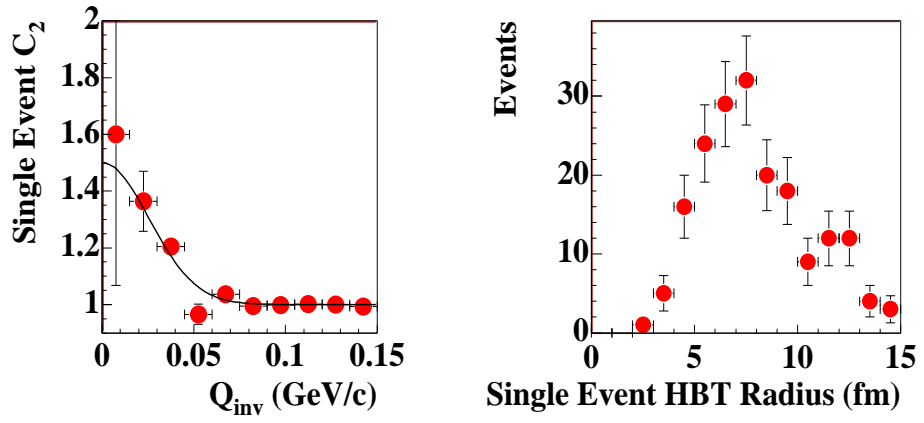


Figure 3: Event by event HBT analysis of central $Pb + Pb$ by NA49 [7], showing a Q_{inv} correlation function and the distribution of the event invariant radius.

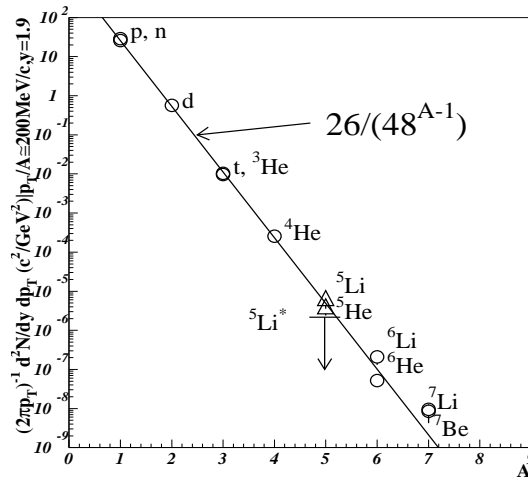


Figure 4: Coalescence yield systematics by E864 [13] for $Au + Au$ at $11 GeV/A$.

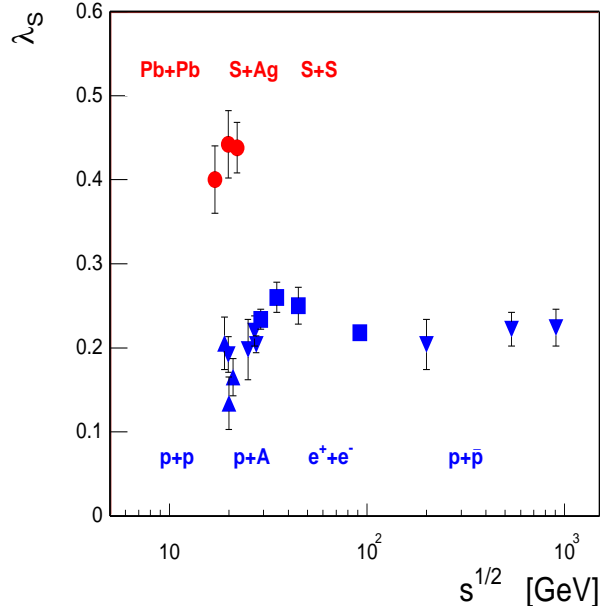


Figure 5: Systematics of the Wroblewski strangeness suppression factor λ_s in elementary collisions and in central nucleus-nucleus collisions at SPS energy [22].

QCD results [20]. This line of argument certainly needs refinement at every step but may serve as a qualitative guideline at least. We would then conclude that a threshold at central $Pb + Pb$, and top SPS energy is characteristic for the J/ψ signal specifically, and that the conditions for the hadron to parton phase change, i.e. $\epsilon = \epsilon_{crit}$, must be reached at more peripheral $Pb + Pb$ collisions, or in central mass 200 collisions at lower \sqrt{s} . Insofar as hadronic observables are sensitive to the phase change they should exhibit a step, kink or such, roughly speaking between $p + p$, $p + A$ or ${}^4He + {}^4He$ (the former ISR data [21]), and central $Pb + Pb$ at $\sqrt{s} = 17 GeV$.

3.1 Hadron yields

Strangeness production data exhibit such an evolution. Fig. 5 shows the systematics of the so-called Wroblewski ratio $\lambda = 2 \langle s + \bar{s} \rangle / (\langle u + \bar{u} \rangle + \langle d + \bar{d} \rangle)$ of global strange to nonstrange quark content in 4π obtained by Becattini et al. [22] from an analysis of central $Pb + Pb$, $S + Ag$ and $S + S$ collisions at the SPS, and from $p + p$, $p + A$, $e^+ + e^-$ and $p + \bar{p}$. There occurs a jump of about two. This enhancement is most dramatically exhibited by the recent WA97 results concerning hyperon production [23], see Fig. 6 (top) in $Pb + Pb$, with jumps increasing in magnitude with $|s| = 1, 2, 3$ in the midrapidity yield relative to $p + Be$ (confirmed by NA49 for 4π cascade hyperon yields [24]). These enhancements stay constant at $\langle N_{part} \rangle > 100$: the transition must be below. The full range of impact parameters is, however, covered in the same reaction for the relative K/π yield (i.e. $(K^+ + K^-)/(\pi^+ + \pi^-)$) by NA49 [25], and for the ϕ yield per participant by NA50 [26]: see Fig. 6 (bottom). Here we see a smooth increase from

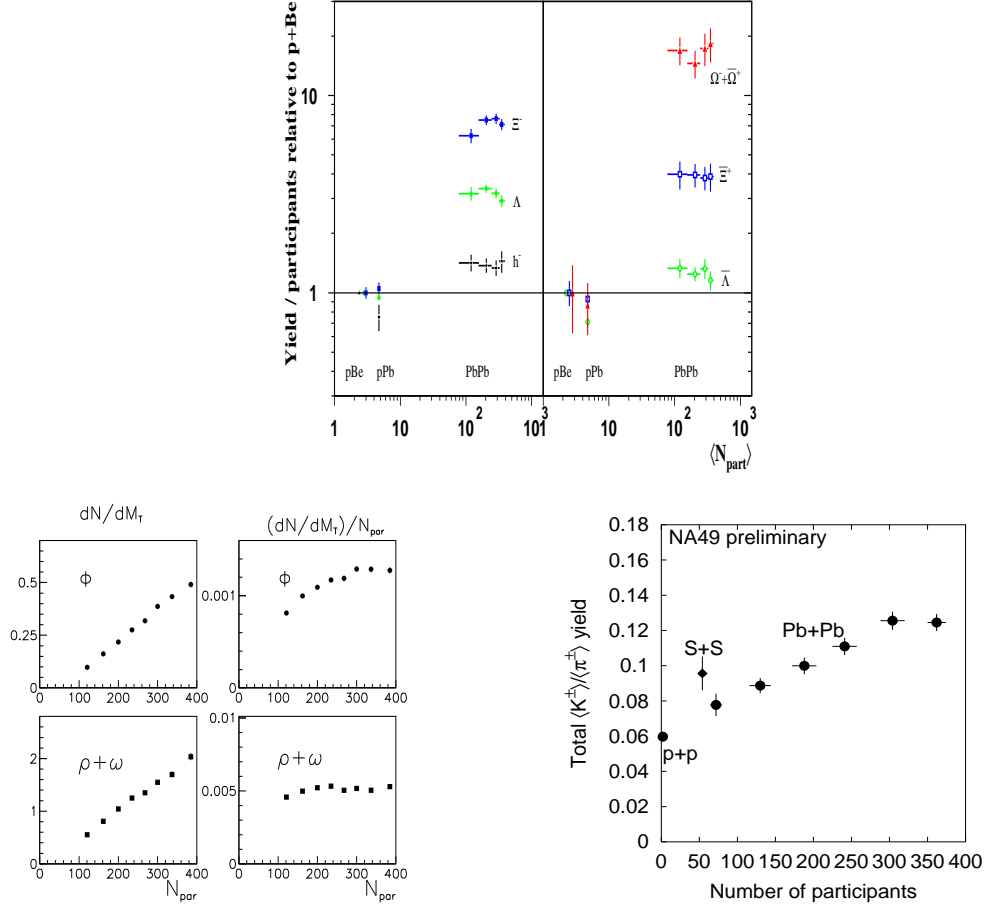


Figure 6: Evolution of hadron production yields with centrality in $Pb + Pb$ collisions at $158 \text{ GeV}/A$. Hyperon data from WA97 [23], vector meson data from NA50 [26] and the K/π ratio from NA49 [25].

pp upwards to $N_{part} \approx 250$ where the ratios flatten out. NA49 shows [27] that overall the ϕ to participant ratio in full 4π increases by a factor of 3.2 whereas the $\langle \phi \rangle / \langle \pi \rangle$ ratio increases by 2.8, and the $\langle K \rangle / \langle \pi \rangle$ ratio by 2.1.

In contrast the nonstrange yields per participant exhibit minor increases only: π/N_{part} and $(\rho + \omega)/N_{part}$ by about 20% [25,26]. NA49 sees a $\langle \bar{p} \rangle / N_{part}$ ratio that is constant [28]. Returning to the J/ψ yield within this systematics Gazdzicki has shown [29] that the ψ/π ratio is constant (about 10^{-6}) from $p+p$ up to minimum bias $Pb+Pb$ ($\langle N_{part} \rangle \approx 100$). NA50 might furnish the continuation of this ratio toward the most central collisions (down by a factor of about 2 to 3 ?).

Overall, the systems of hadronic yield ratios undergoes a dramatic change in going from $p+p$, $p+A$ to central $Pb+Pb$ at $\sqrt{s} = 17 \text{ GeV}$; the changeover occurs at semi-central $Pb + Pb$ and below central $S + heavy nucleus$ (the data are not as comprehensive). At the AGS the trend is similar but less dramatical [30] perhaps due to the lack of hyperon yield systematics. We will return to the hadronic composition of the final state in section

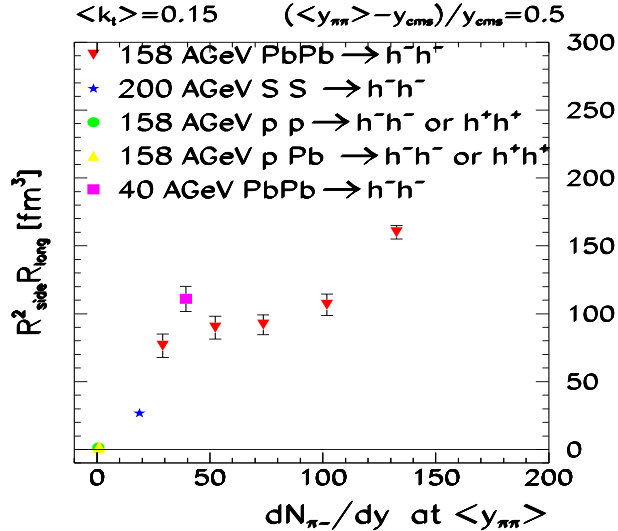


Figure 7: Systematics of the HBT eigenvolume $R_{side}^2 R_{long}$ with negative pion rapidity density near midrapidity for $p + p$, $p + Pb$, $S + S$ and $Pb + Pb$ by NA49 [32].

6, showing that it holds the key to determine the parameters of the parton to hadron phase transformation.

3.2 Bose-Einstein correlations

Data of high precision are now available for the evolution of HBT "geometrical" source parameters with system size (centrality), \sqrt{s} and pair transverse invariant mass, both from the AGS and the SPS experiments. Concerning the evolution with system size the AGS E802/866 Collaboration showed [31] that the parameter R_{side} (which lends itself most directly to characterize the transverse source dimension [4]) is very strictly proportional to the cube root of the participant nucleon number from peripheral $Si + Al$ to central $Au + Au$ collisions. A result augmented by NA49 [32] which considers R_{side} as a function of the cube root of the pion multiplicity density near midrapidity for the sequence $p + p$, $p + Pb$, $S + S$ and $Pb + Pb$ at various impact parameters. These data are shown in Fig. 7.

They include the first result from the SPS trial run at 40 GeV/A for central $Pb + Pb$, the data point sitting somewhat high within the surrounding R_{side} values for semiperipheral $Pb + Pb$ at 158 GeV/A. A feature reminiscent of the similar excursion in the K/π ratio (Fig. 6 bottom) exhibited by the central $S + S$ data point falling above the systematics of participant number dependence in $Pb + Pb$. A possible hint that neither the participant number scale nor the midrapidity density of produced particles (pions) properly reflects the difference of a central collision, at lower A or \sqrt{s} , and the seemingly concurrent, fairly peripheral $Pb + Pb$ collisions. One might suspect the higher net baryon density near midrapidity, or the geometrically more compact primordial interaction volume of central collision to cause this second order effect which deserves further study.

AGS E866 also reports [31] comprehensive data concerning the "duration of emission"

parameter. In terms of the Bertsch-Pratt variables it is given by the square root of $R_{out}^2 - R_{side}^2$ and denotes the temporal width of the source luminosity with regard to decoupling pion pairs. It approaches $4 \text{ fm}/c$ in central $Au + Au$, in close agreement with the former NA49 analysis [33] of central $Pb + Pb$ at the SPS. This parameter highlights the wider informational content of HBT analysis. Beyond the mere spatial geometry of the source, traditionally expected from such data, it elucidates the time scale of source decomposition upon expansion which thus turns out to be very short owing to an "explosive" hadronic expansion dynamics [34]. Actually it is equally short at $\sqrt{s} = 4.3, 8.8$ and 17 GeV [32]. We shall return to this information in section 5, for the discussion of global hadronic freezeout.

Whereas we see a smooth increase of R_{side} and R_{out} with centrality the NA49 minimum bias data [32] indicate a flattening out of the longitudinal radius parameter which is related to the overall reaction time. Like the duration of emission parameter it shows no variation at $40 \text{ GeV}/A$ [32] but is much smaller at AGS $Au + Au$ at $11 \text{ GeV}/A$ [31], a somewhat counterintuitive finding. In any event the two reaction time related parameters indicate no maximum anywhere, including the lower AGS energies 2 to $8 \text{ GeV}/A$ that were analyzed by E895 [35]. They thus give no reason to suspect that the "softest point" of the EOS (i.e. the "position" of the hadron-parton phase transition) has been hit which might reflect in an extended time scale [35,36] due to existence of a long-lived mixed phase. This brings me to the topic of the next section.

4 Evolutions and onset searches in directed flow observables

The occurrence of directed flow phenomena can be linked to the time integral over accelerating forces, carried out over the entire expansions dynamics until freezeout. The forces relate to unisotropic local pressure fields, the pressure in turn results from density and temperature via the equation of state (EOS). Rischke [37] and Shuryak [38,39] have shown repeatedly how various models of a phase transition between a hadronic resonance gas and a schematic quark gluon phase exert their influence via the EOS on directed (ν_1) and elliptic (ν_2) flow of various hadrons. These schematic models focus on the transition "point" resulting in a mixed phase which causes the pressure to fade: the "softest point" of the dynamics which causes a discontinuity in the excitation function of the observable at the "onset" of the new phase. It has often been remarked that the terminology of points and onsets might be misleading as each colliding system features large gradients of energy density in its interior sections: there should be no sudden or pointlike phenomena if a realistic hydrodynamical model is consulted. In fact Schlei [40] reported such calculations with the HYLANDER model which did not confirm sudden effects upon (gradually) crossing the EOS boundary.

Two sets of data emerged as possible candidates for a smooth onset behaviour. The beautiful systematic AGS data, combined from E877 [41] and EOS [30,43] $Au + Au$ provide for an excitation function of directed and elliptic flow, the latter changing sign at about $4 \text{ GeV}/A$. Danielewicz [44] showed that ν_2 may be best reproduced by a transition from a hard ($K = 380 \text{ MeV}$) to a soft ($K = 210 \text{ MeV}$) EOS, occurring between about 2 and $5 \text{ GeV}/A$. A similar smooth effect was pointed out in the NA49 elliptic pion flow data [45] for minimum bias $Pb + Pb$ by Sorge [46] employing RQMD with the microscopic adaptation of a phase transition which leads to a kink in ν_2 at impact parameters from about 6 to 9 fm , not unlike the data. But we are now faced with onset candidates at

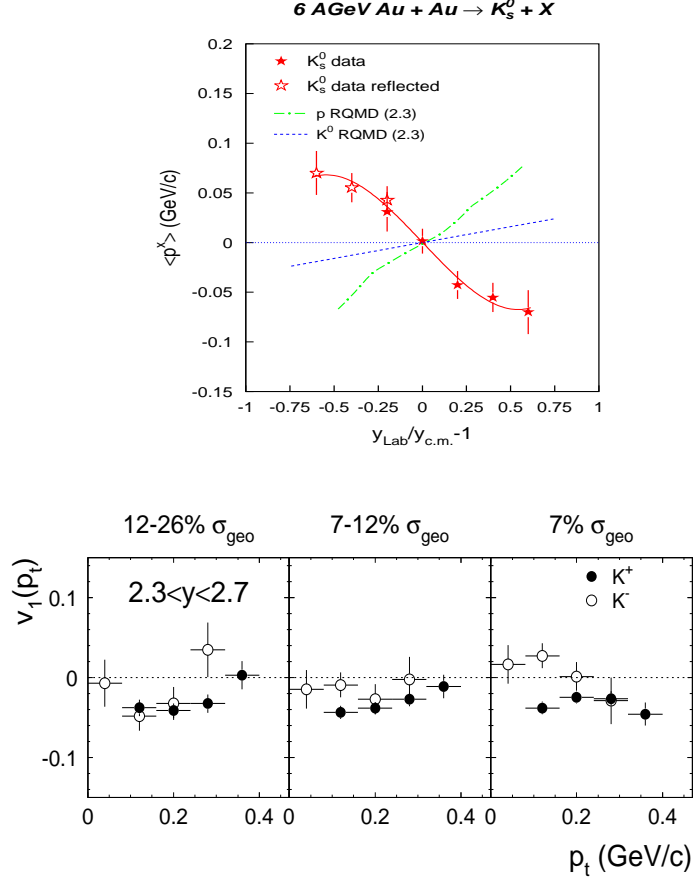


Figure 8: In plane directed flow of K_s^0 as function of cms rapidity in semiperipheral $Au + Au$ at 6 GeV/A by E895 [30] (top) and p_t dependence of K^+ , K^- directed flow at 11 GeV/A by E877 [42].

$E = 4 GeV/A$ and 158 GeV/A , in semi-central mass 200 collisions.

Flow of strange particles offers a different window on the EOS of dense matter. For kaon directed in plane flow we have data at 1-2 GeV/A from SIS [47] and were presented new AGS data for $Au + Au$ shown in Fig. 8: Neutral kaons K_s^0 exhibit a dramatic $\langle p_x \rangle$ signal in the 6 GeV/A E895 data [30] (top) perpendicular to the proton flow (and in striking disagreement with the RQMD (2.3) K^0 prediction) thus pointing to a strongly repulsive in-medium nucleon neutral kaon potential [48] which is baffling because K_s^0 is K^0 and \bar{K}^0 to equal parts. The E877 data [42,49] are for the top AGS energy 11.5 GeV/A and show (bottom Fig. 8) that both K^+ and K^- show very little $\langle p_x \rangle$ throughout (like at SIS energy). As such they also push away from the protons and lambdas but K_s^0 is really anti-correlated to the latter.

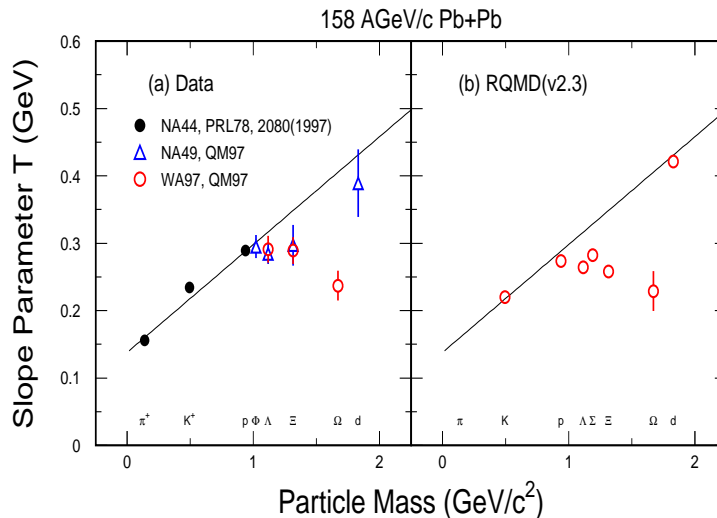


Figure 9: Systematics of hadron inverse slope parameters from pion to deuterium for central $Pb + Pb$, and RQMD results by Nu Xu [54] showing hyperon "excursion".

5 Global freezeout and radial velocity fields

In considering the final phase of hadronic fireball expansion we first focus our attention at the global freezeout: when hadrons decouple from strong interaction (with exception of a few resonances left over which decay even later, during free-streaming). It is known [33,50] that collective velocity fields, both in transverse and (even stronger) in longitudinal direction, dominate the hadronic transverse mass spectra and the pair correlations (in their dependence on m_T). This so-called hadronic radial flow seems at least in part to result from the near isentropic nature of hadronic expansion [6,51], and may have contributions from the pressure during the preceding partonic phase if it exists.

All of this has been discussed already at QM97 but we have new insight into the inverse m_T slope systematics previously established for SPS central $Pb + Pb$ collisions by NA44, NA49 and WA97 [50,52,53]. We illustrate this in Fig. 9.

Nu Xu showed [54] that RQMD (2.3) accounts well for the previously noted excursion of the hyperon m_T -spectral slope parameters, notably for the cascade and omega particles, from the linear increase of T with hadron mass that would result if all hadrons froze out simultaneously from a common radial velocity field. But Nu Xu showed that e.g. the departure of the Ω slope results in RQMD from an early decoupling owing to the small total cross section. After emerging from hadronization the Ω scatters only about once or twice whereas protons undergo about 6 successive, mostly elastic collisions [55]. This offers the tantalizing prospect to determine with low cross section hadrons the transverse flow existing directly near the stage of primordial hadrosynthesis, at which the true temperature is about 170-180 MeV as I shall describe in the next section [22,56,57]. The observed Ω slope $T = 230 MeV$ would then give an estimate of "primordial flow",

from the partonic phase, amounting to $\beta_{\perp} = 0.27$ by using the Heinz formula [58] $T = T_{true} \sqrt{(1 + \beta)/(1 - \beta)}$. Next to the Ω the ϕ would be most interesting in this regard but NA49 and NA50 report a discrepancy here: $T = 295$ and 225 MeV , respectively [26,27].

To determine the freezeout conditions $(T_{true}, \beta_{\perp})$ for the highly abundant hadrons π, K, \bar{p} Sollfrank and Heinz [58] suggested long ago to resolve the T, β_{\perp} ambiguity of each individual fit to the transverse mass spectrum by superimposing the three "corridors" of T, β_{\perp} and looking for their overlap in the T, β_{\perp} plane which they found at $T_{true} = 125 \text{ MeV}$ and $\beta_{\perp} = 0.6$ for SPS sulphur collision data. Note that this procedure does **not** pick out the minimum χ^2 fit values of T, β_{\perp} for individual hadrons which might be **different** as Peitzmann [1] demonstrated for the neutral pion, wide m_T range WA98 data (shown in Fig. 1), also pointing out all the difficulties arising in the pion spectra from resonance feeding, relativistic flow and Croonin effect contributions. It seems advisable to restrict to kaon, proton, antiproton and deuteron spectra in order to pin down the global freezeout conditions.

NA49 has suggested [33] an alternative method combining spectral data with HBT analysis because the hydrodynamically inspired source model [6,51] predicts the transverse HBT radius parameter to fall off with m_T of the pair as

$$R_T(m_T) = R_G \left(1 + \frac{m_T \beta_{\perp}^2}{T}\right)^{-1/2} \quad (1)$$

at midrapidity; here R_G is the "true" transverse radius of the source, and T is the "true" freezeout temperature. The fit of the m_T dependence of R_T then contains another continuous ambiguity, this time R_G vs. β^2/T or β^2 vs. T if R_G gets fixed. Fig. 10 illustrates this procedure [33] for central $Pb + Pb$ collisions. The information from spectra (which implicitly results from total transverse energy conservation [59]) and HBT (transverse coherence length conservation [60]) comes at right angles. NA49 concluded $T = 120 \text{ MeV}$, $\beta_{\perp} = 0.55$ but in the light of the above discussion one might now ignore the negative hadron (i.e. mostly π) information deducing the bulk hadron **freezeout conditions** $T = 110 \pm 10 \text{ MeV}$, $\beta_{\perp} = 0.60 \pm 0.08$ for central $Pb + Pb$ near midrapidity in agreement with Wiedemanns [4] analysis.

The crucial correlation data that enter this quantification of a very strong "flow" phenomenon can be expanded as NA44 showed [61]. Fig. 11 reproduces their compounded data for the pair m_T dependence of pion, kaon and proton two particle Bose (Fermi) correlation and from deuteron coalescence, all for $Pb + Pb$ at $\sqrt{s} = 17 \text{ GeV}$. First data on the m_T dependence of HBT radii in $p + p$ and $p + Pb$ at similar energy were shown by NA49 [32]: some effect is visible (not surprisingly) in the longitudinal radius but the data are inconclusive about the transverse radii at the present level of statistics.

Finally: when does this final freezeout occur? There ought to be a wide spread in decoupling times as the surface of the primordial interaction volume starts emitting hadrons into free streaming right after formation time. From pion pair HBT analysis in the framework of the expanding source model [6,51] one extracts two relevant parameters: the average decoupling time τ and the Gaussian duration of emission width $\Delta\tau$ (see previous section). For central $Pb + Pb$ NA49 deduced [33,56] the values $\tau = 8 \text{ fm}/c$ and $\Delta\tau = 4 \text{ fm}/c$ at midrapidity. Decoupling would thus cease at about $20 \text{ fm}/c$. Sorge [46] has challenged the validity of the thus derived time scale and, in fact, both the RQMD [62] and VNI models [63] put the end of the decoupling phase to about $30 \text{ fm}/c$, in this collision. This needs further discussion.

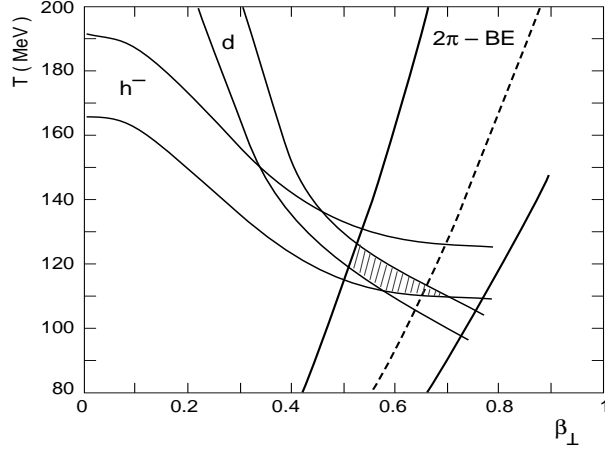


Figure 10: Global freezeout parameters T and β_{\perp} for central $Pb + Pb$ combining m_T spectral information from negative hadrons and deuterons with pion correlation analysis by NA49 [33].

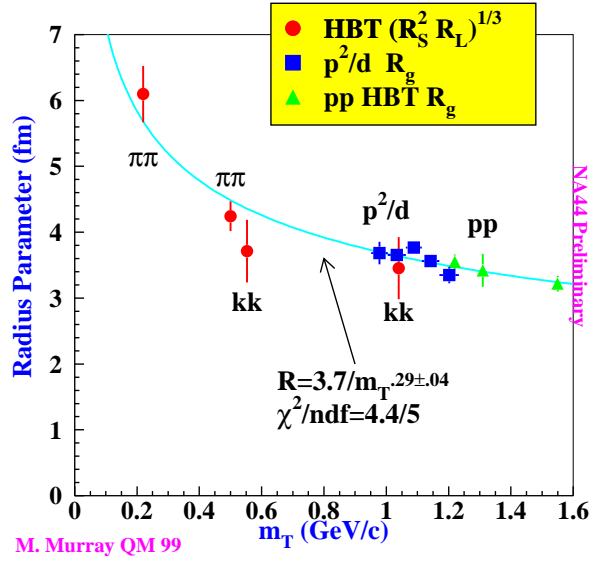


Figure 11: Systematics of m_T dependence for correlation radii from $\pi\pi$, KK , pp and deuteron coalescence in central $Pb + Pb$ collisions by NA44 [61].

6 Primordial hadrosynthesis and the parton-hadron phase transformation

If we, tentatively, accept the hypothesis [64] that the steep drop of the J/ψ yield in the most central $Pb + Pb$ collisions reported at this Conference by NA50 [65] signals a partonic phase which Debye-screens this tightly bound hadron we might conclude that the average energy density amounts to about 3 times the critical density ϵ_c of the QCD deconfinement transition. In section 3 we have hence argued that $\epsilon_c \approx 1 GeV/fm^3$ invoking the Bjorken estimate $\epsilon = 3 GeV/fm^3$ obtained for central $Pb + Pb$ collisions [19]. One then expects to receive signals specific to the exit from this phase, i.e. from the bulk parton to hadron phase transformation bound to occur once the primordial high energy density state expands and cools toward ϵ_c and T_c . Determination of these critical parameters is the principal goal of our research (perhaps adding the need to specify the order of this phase transformation).

In this section I shall argue that the set of bulk hadronic production rates and ratios is a direct consequence of this parton to hadron phase transformation, occurring in central $Pb + Pb$ collisions at top SPS energy, and perhaps already in central $S + S$ mass 200 collisions. In spite of the evidence discussed in the last sections for an extensive dynamical evolution and collective expansion of the fireball I argue that its chemical composition is hardly changed by **inelastic** hadronic final state interactions [55]. The observed hadron yields thus reflect the primordial conditions at the parton to hadron phase transition, i.e. the critical values T_c and ϵ_c and, moreover, the flavour composition at the end of the partonic phase. This view [56] was suggested by hadrochemical model studies [22,58,66] of hadron production ratios, as confronted by models of parton hadronization [63,67]. It was extensively discussed by Heinz at this Conference [57]. It is based on a coherent analysis of three seemingly separate investigations of hadron production data.

Firstly, Ellis and Geiger [68] developed in 1996 a partonic transport model for the analysis of LEP data concerning W and Z decay to hadrons at $\sqrt{s} \approx 90 GeV$. The model (known now as VNI) consists of an initialization step creating an initial quark-gluon population that is evolved in a QCD partonic transport mode which, in turn, ends in a coalescence phase creating colour singlet pre-hadronic resonances that decay into the observed hadrons. Good overall agreement was obtained with the data comprising all hadronic yields up to hyperons. Most importantly the authors noted a remarkable insensitivity of the yield distribution to the detailed assumptions made in the model concerning the non-perturbative mechanisms of hadronization. They concluded that the statistical phase space weights of the various hadronic species overwhelm all other microscopic influences, and that the final multi-hadronic population distribution thus represents the **maximum entropy** state of highest probability.

Secondly, it is therefore not surprising that thermal hadro-chemistry models of Hagedorn-type successfully describe the same LEP data. Becattini [69] employed a canonical partition function showing that the multihadronic state represented a "hadrochemical family" characterized by only two essential parameters, a temperature $T = 165 MeV$ and a strangeness under-saturation factor $\gamma_s = 0.65$. As there is no inelastic hadronic rescattering whatsoever in such Z, W decays it was obvious that such an ordered state of hadrons could not result from any equilibrating interaction at the hadronic side. The statistical order is created **from above**, i.e. from higher energy density prevailing at the onset of hadronization, at the critical QCD energy density ϵ_c . Arriving at the hadronic side of the phase transformation this state is partially out of proper hadronic chemical equilibrium as indicated by $\gamma_s < 1$. The preceding partonic phase enters its specific

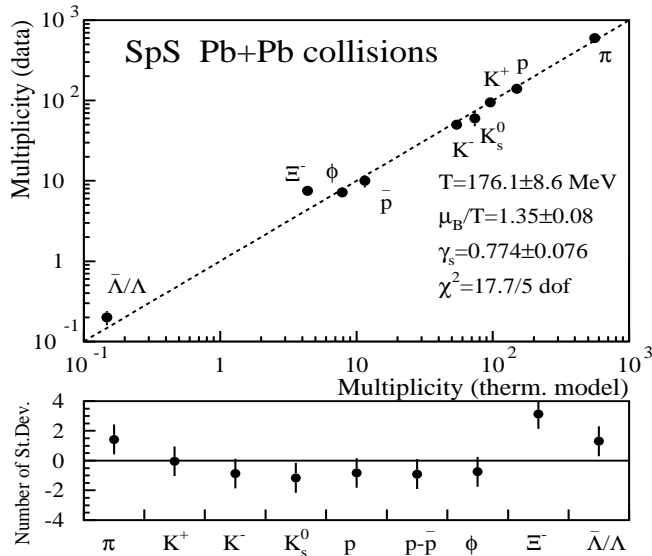


Figure 12: Grand canonical thermal model analysis of hadron yields and yield ratios in central $Pb + Pb$ collisions by Becattini [70]. Preliminary data from NA49 [25].

strange quark/antiquark population (which may or may not represent a flavour equilibrium at the partonic level) into the hadronization process which creates essentially no new strangeness but plenty of light quarks. The emerging hadronic population thus appears strangeness-undersaturated at the transition temperature, and it can not readjust the strangeness population owing to its own proper "explosive" expansion [55,56]. It thus preserves the signatures of the phase transition, which freeze out at the instant of hadronization.

Thirdly, it turns out that the multihadronic population order observed in central $Pb + Pb$ collisions can be understood similarly as a fingerprint of the parton to hadron phase transformation [56,57,66,67,69,71]. However, we must expect significant differences in detail proceeding from the outcome of LEP $e^+ + e^-$ data analysis to central $Pb + Pb$ collisions. Recall that the hadronic population ratios were shown in section 3 to exhibit a dramatic evolution in proceeding from $p + p$ via minimum bias $Pb + Pb$, to finally settle into a new pattern becoming stationary from semi-central collisions onward (Fig. 6) to central $Pb + Pb$ at the top SPS energy. There seems to occur a transition from hadron population patterns characteristic of elementary $e^+ + e^-$, $p + p$, $p + \bar{p}$ collisions at $\sqrt{s} \geq 20$ GeV to central $Pb + Pb$ at the same energy. The hadrochemical model analysis reflects this transition in its proper parameters T , γ_s and baryochemical potential μ_B but again leads to a perfect fit of the hadronic production ratios.

Figs. 12 and 13 illustrate the recent analysis of $Pb + Pb$ central collision data by Becattini [70] and by Braun-Munzinger et al. [66]. The former analysis refers to NA49 data only whereas the latter includes an interpolation of all available data from NA44, NA49 and WA97. Both models employ the grand canonical version of the thermodynamical equilibrium model but differ in detail (concerning employment of γ_s and hadron

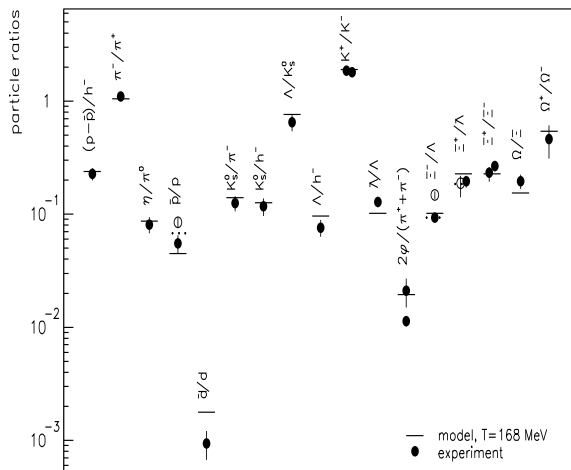


Figure 13: Thermal model analysis by Braun-Munzinger et al. [66] for central $Pb + Pb$ hadron yields compiled from NA44, 49 and WA97.

eigenvolume corrections). However the outcome agrees rather closely: Becattini derives $T = 176 \pm 9 \text{ MeV}$, $\mu_B = 237 \pm 20 \text{ MeV}$, $\gamma_s = 0.77 \pm 0.08$ and Braun-Munzinger et al. get $T = 170 \pm 10 \text{ MeV}$, $\mu_B = 270 \text{ MeV}$ and $\gamma_s = 1$ (the latter a fixed parameter in this analysis). Thus, in comparison to the $e^+ + e^-$ hadronization results, the temperature of primordial hadronization may be slightly higher, the baryochemical potential (near zero in elementary collisions) acquires prominence by the presence of an excess of light quarks over light antiquarks, due to the stopped-down initial high valence quark density in the participating nuclear matter. Most prominently the strangeness undersaturation, characteristic of elementary collisions (Fig. 5) fades away. This is not resulting from any inelastic equilibration at the hadronic side of the phase transformation which does not take place owing to the "explosive" expansion cooling of the interaction volume as Heinz has shown [55,56,57]. The hadronic expansion mode is governed by elastic interactions which produce the near isentropic "flow" mode generating the collective velocity fields that I described in section 5. The hadronic composition thus freezes out immediately at the instant of hadronization, the chemical composition being out of thermal equilibrium ever after. The apparent fading of the strangeness suppression factor γ_s (which leads to the various levels of strange hadron yield enhancement, in comparison to elementary collisions) must, therefore, stem from the **partonic** phase flavour balance (as was demonstrated by Zimanyi [71] at this conference), entering a higher primordial strangeness saturation level into the hadronization transition. In fact Sollfrank et al. [72] have shown that the observed $s + \bar{s}$ density is compatible with hadronization from a flavour equilibrated quark-gluon plasma at $T \approx 180 \text{ MeV}$.

We thus seem to narrow in onto the most cherished topic of the field: pinning down

the parameters of the parton to hadron phase transformation. This was the highlight of QM99 as far as hadronic signals are concerned. As for a summary of the considerations that lead to this conclusion I chose to give U. Heinz [57] the last word: "The analysis of soft hadron production data at the SPS indicates that hadron formation proceeds by statistical hadronization from a prehadronic state of deconfined quarks. This leads to pre-established apparent chemical equilibrium among the formed hadrons at the confinement temperature T_c ; it is not caused by kinetic equilibration through hadronic rescattering. After hadronization the hadron abundances freeze out more or less immediately. The chemical freeze out temperature thus coincides with the critical QCD temperature, $T_{chem} \approx T_c \approx 170 - 180 \text{ MeV}$ (at $\mu_B \approx 250 \text{ MeV}$), corresponding to a critical energy density $\epsilon_c \approx 1 \text{ GeV}/fm^3$ as predicted by lattice QCD".

References

- [1] Th. Peitzmann, these Proceedings;
Ch. Blume, PhD Thesis, Univ. Münster (1998).
- [2] B. Lenkeit, these Proceedings.
- [3] M. Gyulassy, these Proceedings.
- [4] U. A. Wiedemann, these Proceedings.
- [5] M. Lisa, these Proceedings.
- [6] S. V. Akkelin and Yu. M. Sinyukov, Phys. Lett. B356 (1995) 525;
U. A. Wiedemann, P. Scotto and U. Heinz, Phys. Rev. C53 (1996) 918;
T. Csörgö and B. Lörstad, Phys. Rev. C54 (1996) 1390.
- [7] G. Roland, private communication.
- [8] H. Appelshäuser, PhD Thesis, GSI, DISS 97-02
- [9] D. Ferenc, CERN ALICE note 93-14;
R. Stock, Proc. NATO Divonne Workshop 1994, Editors J. Letessier, H. Gutbrod
and J. Rafelski.
- [10] A. Mekjan, Phys. Rev. Lett. 38 (1977) 640.
- [11] I. Bearden, these Proceedings.
- [12] E866 Collaboration, private communication.
- [13] G. van Buren, these Proceedings.
- [14] G. Ambrosini et al., NA52 Coll., Nucl. Phys. A638 (1998) 411c.
- [15] E. Finch, these Proceedings.
- [16] L. Kluberg, these Proceedings.
- [17] T. Matsui and H. Satz, Phys. Lett. B178 (1986) 416.
- [18] E. Laerman, Nucl. Phys. A610 (1996) 1c.

- [19] T. Alber et al., NA49 Coll., Phys. Rev. Lett. 75 (1975) 3814;
M. Aggarwal et al., WA98 Coll., Nucl. Phys. A610 (1996) 200c.
- [20] F. Karsch, Nucl. Phys. A590 (1995) 367c.
- [21] H. G. Fischer, Z. Phys. C38 (1988) 105.
- [22] F. Becattini, M. Gazdzicki and J. Sollfrank, Nucl. Phys. A638 (1998) 403c.
- [23] E. Andersen et al., WA97 Coll., Phys. Lett. B433 (1998) 209;
F. Antinori, these Proceedings.
- [24] H. Appelshäuser et al., NA49 Coll., Phys. Lett. B444 (1998) 523.
- [25] F. Sikler, these Proceedings.
- [26] N. Willis, these Proceedings.
- [27] C. Höhne, these Proceedings.
- [28] G. I. Veres, these Proceedings.
- [29] M. Gazdzicki and M. I. Gorenstein, hep-ph/9905515 to be published in Acta Phys.
Pol.
- [30] G. Rai, these Proceedings.
- [31] R. Solz, these Proceedings.
- [32] R. Ganz, these Proceedings.
- [33] H. Appelshäuser et al., NA49 Coll., Eur. Phys. J. C2 (1998) 661.
- [34] J. Letessier, J. Rafelski and A. Tounsi, Nucl Phys. A590 (1995) 613c.
- [35] S. Pratt, Phys. Rev. C33 (1986) 1314.
- [36] G. F. Bertsch, Nucl. Phys. A498 (1989) 173c.
- [37] D. H. Rischke, Nucl. Phys. A610 (1996) 88c.
- [38] E. V. Shuryak, Nucl. Phys. A638 (1999) 207c.
- [39] E. V. Shuryak, these Proceedings.
- [40] B. Schlei, these Proceedings.
- [41] J. Barette et al., E877 Coll., Nucl. Phys. A638 (1998) 69c.
- [42] K. Filimonov, these Proceedings.
- [43] H. Liu et al., E895 Coll., Nucl. Phys. 638 (1998) 451c.
- [44] P. Danielewicz, these Proceedings.
- [45] A. M. Poskanzer, these Proceedings.
- [46] H. Sorge, these Proceedings.
- [47] Y. Shin et al., KaoS Coll., Phys. Rev. Lett. 81 (1998) 1576.

- [48] G. Q. Li et al., Phys. Lett. B329 (1994) 149.
- [49] J. Barette, these Proceedings.
- [50] I. G. Bearden et al., NA44 Coll. Nucl. Phys. A638 (1998) 103c.
- [51] J. D. Bjorken, Phys. Rev. D27 (1983) 140; U. Heinz, Nucl. Phys. A610 (1996) 264c.
- [52] H. Appelshäuser et al., NA49 Coll., Phys. Rev. Lett. 82 (1999) 2471.
- [53] D. Elia, these Proceedings;
R. Lietava et al., WA97 Coll., J. Phys. G25 (1999) 181.
- [54] Nu Xu, these Proceedings.
- [55] A. Dumitru et al., nucl-th/9901046;
S. Bass et al., nucl-th/9902062.
- [56] R. Stock, Phys. Lett. B456 (1999) 277.
- [57] U. Heinz, these Proceedings, nucl-th/9907060.
- [58] J. Sollfrank and U. Heinz, in Quark Gluon Plasma 2,
R. Hwa (Ed.), World Scientific.
- [59] R. Stock, Nucl. Phys. A630 (1998) 535c.
- [60] T. Csörgö and B. Lörstadt, Nucl. Phys. A590 (1995) 465c.
- [61] M. Murray, these Proceedings.
- [62] H. Sorge, Phys. Lett. B373 (1996) 16.
- [63] K. Geiger, Nucl. Phys. A638 (1998) 551c;
K. Geiger and D. K. Srivastava, Phys. Rev. C56 (1997) 2718.
- [64] H. Satz, these Proceedings.
- [65] C. Cicalo, these Proceedings.
- [66] P. Braun-Munzinger, I. Heppe, J. Stachel, nucl-th/9903010, to appear in Phys. Lett. B;
J. Stachel, these Proceedings.
- [67] W. Bartz, B. L. Friman, J. Knoll and H. Schultz, Nucl. Phys. A519 (1990) 831.
- [68] J. Ellis and K. Geiger, Phys. Rev. D54 (1996) 1967.
- [69] F. Becattini, Z. Phys. C69 (1996) 485, and hep-ph/9701275.
- [70] F. Becattini, private communication.
- [71] J. Zimanyi, these Proceedings;
J. Zimanyi, T. S. Biro and P. Levai, hep-ph/9904501.
- [72] J. Sollfrank, F. Becattini, K. Redlich and H. Satz, Nucl. Phys. A638 (1998) 399c.